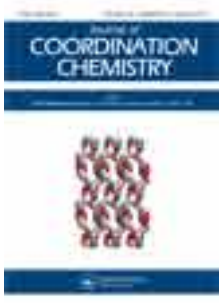

Journal of Coordination Chemistry
Publication details, including instructions for authors and subscription information:
http://www.tandfonline.com/loi/gcoo20

Synthesis, spectroscopic characterization, in vitro cytotoxic and structure activity relationships of some mononuclear Ru(II) complexes

Sreekanth Thota [a], Srujana Vallala [a], Mohammad Imran [a], Sravani Mekala [a], Shyam Sunder Anchuri [a], Subhas Somalingappa Karki [b], Rajeshwar Yerra [a], Jan Balzarini [c] & Erik De Clercq [c]

[a] Department of Pharmaceutical Chemistry & Toxicology, SR College of Pharmacy, Warangal, India

[b] Department of Pharmaceutical Chemistry, KLE University's College of Pharmacy, Bangalore, India

[c] Rega Institute for Medical Research, Katholieke Universiteit Leuven, Leuven, Belgium

Accepted author version posted online: 04 Feb 2013.Published online: 25 Mar 2013.

To cite this article: Sreekanth Thota , Srujana Vallala , Mohammad Imran , Sravani Mekala , Shyam Sunder Anchuri , Subhas Somalingappa Karki , Rajeshwar Yerra , Jan Balzarini & Erik De Clercq (2013): Synthesis, spectroscopic characterization, in vitro cytotoxic and structure activity relationships of some mononuclear Ru(II) complexes, Journal of Coordination Chemistry, 66:6, 1031-1045

To link to this article: http://dx.doi.org/10.1080/00958972.2013.773318

Journal of Coordination Chemistry
Vol. 66, No. 6, 20 March 2013, 1031–1045

Synthesis, spectroscopic characterization, *in vitro* cytotoxic and structure activity relationships of some mononuclear Ru(II) complexes

SREEKANTH THOTA*†, SRUJANA VALLALA†, MOHAMMAD IMRAN†, SRAVANI MEKALA†, SHYAM SUNDER ANCHURI†, SUBHAS SOMALINGAPPA KARKI‡, RAJESHWAR YERRA†, JAN BALZARINI§ and ERIK DE CLERCQ§

†Department of Pharmaceutical Chemistry & Toxicology, SR College of Pharmacy, Warangal, India
‡Department of Pharmaceutical Chemistry, KLE University's College of Pharmacy, Bangalore, India
§Rega Institute for Medical Research, Katholieke Universiteit Leuven, Leuven, Belgium

(*Received 28 December 2011; in final form 29 November 2012*)

New mononuclear Ru(II) complexes $[Ru(A)_2(B)]^{2+}$, where A = 2,2′-bipyridine/1,10-phenanthroline and B = 3,4,5-tri-OCH_3-DPC, 4-CH_3-DPC, 4-$N(CH_3)_2$-DPC, 4-NO_2-DPC, N-BITSZ, PTSZ and PINH, were prepared and characterized by spectroscopic methods. The *in vitro* cytotoxic activities of the complexes and their corresponding ligands were investigated against the human cancer T-lymphocyte cell lines molt 4/c8 and CEM and the murine tumor leukemia cell line L1210, human promyelocytic leukemia cells (HL-60) and Bel-7402 liver cancer cells by MTT assay. The complexes $[Ru(A)_2(B)]^{2+}$ (A = 1,10-phenanthroline, B = 3,4,5-tri-OCH_3-DPC) exerts rather more potent activities against all of these cell lines, especially for CEM and L1210. Ru complexes and structure–activity relationships and anticancer mechanisms are also discussed.

Keywords: Ruthenium complexes; MTT; Structure-activity relationship

1. Introduction

Ruthenium complexes are widely used in bioinorganic chemistry, organometallic chemistry [1–8] and in medicine [9, 10]. The properties of ruthenium complexes can be altered by choice of ligand for multiple applications [11–14]. Ruthenium complexes have many biological and pharmacological activities, including anticancer [9], antioxidant [15, 16], antibacterial [17–20], antifungal [19, 20], antiviral [6], antimalarial [21], and cytotoxicity [22].

Ruthenium complexes having the general formula $[Ru(S)_2(U)]$, where S = 2,2′-bipyridine/1,10-phenanthroline and U = tpl, 4-Cl-tpl, 4-CH_3-tpl, 4-OCH_3-tpl, 4-NO_2-tpl and pai provide examples [4]. The most prominent examples, Na(trans-$RuCl_4$(DMSO)(imid)] NAMI and its more stable imidazolium complexes [Indit][trans-$RuCl_4(ind)_2$], KP1019

*Corresponding author. Email: srph_office@yahoo.co.in

ISSN 0095-8972 print/ISSN 1029-0389 online © 2013 Taylor & Francis
http://dx.doi.org/10.1080/00958972.2013.773318

show high selectivity for tumor metastasis [23, 24] and low toxicity at pharmacologically active doses [25–27], successfully completing phase-I clinical trials [28].

Ruthenium(II) arene complexes show cytotoxic properties *in vitro* as well as *in vivo* [29, 30]. A series of complexes [Ru(n6-arene)Cl(en)](PF6), en = ethylene diamine, arene = benzene, p-cymene, tetrahydroanthracene, etc. have been studied for their *in vitro* anticancer activity [31]. We recently reported certain Ru(II) complexes that are sufficiently stable under physiological conditions and possess excellent antitumor cytotoxic activity towards human cell lines [32].

Our research has focused on $[Ru(A)_2(B)]^{2+}$, where A = 2,2′-bipyridne/1,10-phenanthroline, B = aryl substituted phenyl hydrazones, and their anticancer activities against transplantable murine tumor cell line, Ehrlich ascitic carcinoma. The *in vitro* cytotoxic activities of these complexes and their corresponding Nitrogen, Sulphur, and Oxygen containing ligands were investigated against human cancer T-lymphocyte cell lines molt 4/C8 and CEM, the murine tumor leukemia cell line L1210, human oral epidermoid carcinoma KB cells, human promyelocytic leukemia cells (HL-60), and Bel-7402 liver cancer cells by MTT assay.

2. Experimental

2.1. *General chemicals*

AR grade solvents and reagents were purchased commercially from E.Merck, Mumbai and S.D. Fine Chem., Mumbai. Hydrated ruthenium trichloride was purchased commercially from Loba Chemie, Mumbai and used without purification. UV–Visible (UV–vis) absorption spectra were recorded on a Shimadzu UVPC-3000 spectrophotometer. FTIR spectra were recorded in KBr powder on a Jasco V410 FTIR spectrophotometer by diffuse reflectance technique. ^{1}H-NMR and ^{13}C-NMR spectra were measured in DMSO-d_6 and $CDCl_3$ on a Bruker Ultraspec 500 MHz/AMX 400/300 MHz spectrophotometer. The chemical shifts are reported against that of TMS. FAB-mass spectra were recorded on a JEOL JMS600 spectrometer with 3-nitro benzyl alcohol as matrix. Microanalyses were carried out on an Elementar Vario elemental analyser. Pyrazoline derivatives were prepared according to the literature method [33, 34].

2.2. *Synthesis of 3-phenyl-5-(1H-pyrrol-2-yl)-4,5-dihydro-1H-pyrazole-1-carbothioamide (PCT)*

2.2.1. Preparation of chalcones (benzylidene acetophenone or 1,3-diphenyl prop-2-en-1-one). A solution of 22 g of sodium hydroxide in 200 mL of water and 125 mL ethanol is placed in a 500 mL bolt head flask provided with a mechanical stirrer [33]. The flask is immersed in an ice bath, 52 g (0.43 M) of freshly distilled acetophenone is added, the stirrer started, and then, 46 g (44 mL, 0.43 M) of pure benzaldehyde added. Keeping the temperature at 25 °C (15–30 °C), stir vigorously until the mixture is so thick that stirring is no longer effective (2–3 h). The stirrer is removed and the reaction mixture left in an ice-chest or refrigerator overnight. The product is collected by filtration, washed with cold water until the washings are neutral to litmus and then with 20 mL of ice-cold ethanol. The crude chalcone (88 g), after drying in air, melts at 50–54 °C. The crude product was recrystallized from ethanol at 50 °C (about 5 mL/g).

2.2.2. Synthesis of 3-phenyl-5-(1*H*-pyrrol-2-yl)-4,5-dihydro-1*H*-pyrazole-1-carbothioamide. To solution of chalcone derivatives (0.01 M) and thiosemicarbazide (0.012 M) in 25 mL of ethanol, a solution of sodium hydroxide (0.025 M) in 5 mL of water was added and refluxed for 8 h [34]. The products were poured into crushed ice and the solid mass which separated was filtered, dried, and recrystallized from appropriate solvents.

2.3. *Preparation of cis-[bis (A) dichlororuthenium(II)] cis-[Ru(A)$_2$Cl$_2$] (where A = 2,2'-bipyridine/1,10-phenanthroline)*

In a round bottom flask fitted with a reflux condenser $RuCl_3 \cdot H_2O$, 1 g (2.5 mM) and ligand A (5 mM) were added [22]. The mixture was refluxed in DMF (50 mL) for 3–4 h under nitrogen. The reddish brown color of the solution slowly turned purple and precipitation of the product occurs. The solution was cooled to room temperature and left overnight at 0 °C. A fine microcrystalline mass was filtered off, repeatedly washed with 30% LiCl solution and dried. The crude solid was purified by recrystallization from anhydrous alcohol to give crystals.

2.4. *General procedure for preparing [Ru(A)$_2$(B)Cl$_2$] (where A = 2,2-bipyridine/1,10-phenanthroline; B = 3,4,5-tri-OCH$_3$-DPC, 4-CH$_3$-DPC, 4-N-(CH$_3$)$_2$-DPC, 4-NO$_2$-DPC, N-BITSZ, PTSZ and PINH)*

To the black microcrystalline *cis*-$Ru(A)_2Cl_2$ (2 mM), excess of ligand B (2.5 mM) was added and refluxed in anhydrous ethanol under nitrogen. The initial colored solution slowly changed to brownish orange at the end of the reaction, which was verified by TLC on silica plates. Excess ethanol was distilled off and silica gel (60–120 mesh) added to this solution. The final complex was purified by column chromatography using silica gel as stationary phase and chloroform–methanol as mobile phase.

2.4.1. [Ru(phen)$_2$(3,4,5-tri-OCH$_3$-DPC)]Cl$_2$. 44%, black crystals, IR (KBr) cm^{-1}: 3483-NH_2, 3040 (C–H), 2946 (C–H), 1610 (C=C), 1324 (C==S). Calcd for $C_{43}H_{37}Cl_2N_7O_3Ru_1S_1$: C, 57.14; H, 4.13; N, 10.85. Found: C, 57.02; H, 4.09; N, 10.69%. ^{1}H NMR (DMSO-d$_6$): δ ppm: 8.84 (s, 1H), 8.72 (d, 2H), 8.49 (d, J = 4.9 Hz, 2H), 8.42–8.31 (d, J = 5.0 Hz, 2H), 8.23 (s, 1H), 8.21 (s, 1H), 8.04–7.94 (d, 4H), 7.83 (s, 1H), 7.76 (d, J = 14.6 Hz, 2H), 7.68–7.58 (m, 4H), 7.57–7.54 (m, 2H), 6.94 (d, 2H), 6.48 (d, 2H), 3.83 (OCH_3, 3H), 3.78 (OCH_3, 3H), 3.76 (OCH_3, 3H), 3.21 (d, 2H). ^{13}C-NMR (d$_6$-DMSO) 159.96–43.82 (43 C). FAB-MS (mNBA): 903 [Ru(phen)$_2$(3,4,5-tri-OCH_3-DPC)]$^{2+}$(Cl$_2$)$^-$; 832 [Ru(phen)$_2$(3,4,5-tri-OCH_3-DPC)]$^{2+}$; 461 [Ru(phen)$_2$]; 371 [3,4,5-tri-OCH_3-DPC].

2.4.2. [Ru(bpy)$_2$(3,4,5-tri-OCH$_3$-DPC)]Cl$_2$. 42%, black crystals, IR (KBr) cm^{-1}: 3510-NH_2, 3050 (C–H), 2958 (C–H), 1639 (C=O), 1320 (C==S). Calcd for $C_{39}H_{37}Cl_2N_7O_3Ru_1S_1$: C, 54.73; H, 4.36; N, 11.46. Found: C, 54.64; H, 4.29; N, 11.42%. ^{1}H NMR (DMSO-d$_6$): δ ppm: 8.26 (s, 1H), 8.15 (d, 2H). 8.02–7.96 (d, J = 4.9 Hz, 2H), 7.94–7.92 (d, J = 5.0 Hz, 2H), 7.86–7.80 (d, 2H), 7.74–7.52 (d, 2H), 7.46–7.45 (d, 2H), 7.44 (d, 2H), 7.37 (s, J = 14.6 Hz, 1H), 7.22–7.00 (m, 4H), 6.75 (d, 2H), 6.4–5.90

(d, 2H), 3.91–3.88 (OCH_3, 3H), 3.84–3.82 (OCH_3, 3H), 3.81–3.80 (OCH_3, 3H), 3.16–3.14 (d, 2H), 3.07 (s, 1H), 2.32 (s, 1H). ^{13}C-NMR (d_6-DMSO) 174.22–54.82 (39 C). FAB-MS (mNBA): 855 $[Ru(bpy)_2(3,4,5\text{-tri-}OCH_3\text{-DPC})]^{2+}(Cl_2)^-$; 784 $[Ru(bpy)_2(3,4,5\text{-tri-}OCH_3\text{-DPC})]^{2+}$; 413 $[Ru(bpy)_2]$; 371 [3,4,5-tri-OCH_3-DPC].

2.4.3. $[Ru(phen)_2(4\text{-}CH_3\text{-DPC})]Cl_2$. 44%, black crystals, IR (KBr) cm^{-1}: 3460 (NH_2), 3068 (C–H), 2946 (C–H), 1640 (C=O), 1347 (C==S). Calcd for $C_{41}H_{33}Cl_2N_7Ru_1S_1$: C, 59.49; H, 4.02; N, 11.84. Found: C, 59.36; H, 4.00; N, 11.78%. ^{1}H NMR (DMSO-d_6): δ ppm: 8.86 (s, 1H), 8.83 (s, 1H), 8.80 (s, J = 4.9 Hz, 1H), 8.56 (d, J = 8.4 Hz, 2H), 8.38 (d, 2H), 8.06 (d, 2H), 7.94 (d, J = 5.0 Hz, 2H), 7.86 (d, 2H), 7.58 (d, 2H), 7.46 (d, 3H), 7.32 (d, 2H), 7.28 (d, J = 14.6 Hz, 2H), 7.25 (d, 2H), 7.18 (d, 2H), 6.25 (d, 2H), 3.86 (s, 1H), 3.82 (s, 1H), 2.35 (s, 3H). ^{13}C-NMR (d_6-DMSO) 168.48–22.14 (41 C). FAB-MS (mNBA): 827 $[Ru(phen)_2(4\text{-}CH_3\text{-DPC})]^{2+}(Cl_2)^-$; 756 $[Ru(phen)_2(4\text{-}CH_3\text{-DPC})]^{2+}$; 461 $[Ru(phen)_2]$; 295 [4-CH_3-DPC].

2.4.4. $[Ru(bpy)_2(4\text{-}CH_3\text{-DPC})]Cl_2$. 44%, black crystals, IR (KBr) cm^{-1}: 3480 (NH_2), 3100 (C–H), 2978 (C–H), 1680 (C=O), 1326 (C==S). Calcd for $C_{37}H_{33}Cl_2N_7Ru_1S_1$: C, 56.99; H, 4.27; N, 12.57. Found: C, 56.81; H, 4.22; N, 12.38%. ^{1}H-NMR (DMSO-d_6): δ ppm: 8.93 (s, 1H), 8.59 (s, 1H), 8.48 (s, J = 4.9 Hz, 1H), 8.26 (d, J = 8.4 Hz, 2H), 8.14 (s, 1H), 7.98 (d, 2H), 7.60 (d, J = 5.0 Hz, 2H), 7.24 (d, 2H), 7.18 (d, 2H), 7.14 (d, 2H), 6.94 (d, 2H), 6.80 (d, J = 14.6 Hz, 2H), 6.74 (d, 2H), 6.28 (d, 2H) 6.18 (d, 2H), 3.90 (s, 1H), 3.83 (s, 1H), 2.56 (s, 2H), 2.34 (s, 3H). ^{13}C-NMR (d_6-DMSO) 172.6–24.28 (37 C). FAB-MS (mNBA): 779 $[Ru(bpy)_2(4\text{-}CH_3\text{-DPC})]^{2+}(Cl_2)^-$; 708 $[Ru(bpy)_2(4\text{-}CH_3\text{-DPC})]^{2+}$; 413 $[Ru(bpy)_2]$; 295 [4-CH_3-DPC].

2.4.5. $[Ru(phen)_2(4\text{-}N(CH_3)_2\text{-DPC})]Cl_2$. 44%, black crystals, IR (KBr) cm^{-1}: 3421 (NH_2), 3155 (C–H), 2985 (C–H), 1680 (C=O), 1336 (C=S). Calcd for $C_{42}H_{36}Cl_2N_8Ru_1S_1$: C, 58.87; H, 4.23; N, 13.08. Found: C, 58.72; H, 4.19; N, 13.04%. ^{1}H NMR (DMSO-d_6): δ ppm: 9.01 (s, 1H), 8.98 (s, 1H), 8.84 (s, J = 4.9 Hz, 1H), 8.76 (d, J = 8.4 Hz, 2H), 8.44 (d, 2H), 8.36 (d, 2H), 8.24 (d, J = 5.0 Hz, 2H), 8.16 (d, 2H), 8.04 (d, 2H), 7.98 (d, 3H), 7.82 (d, 2H), 7.83 (d, J = 14.6 Hz, 2H), 7.64 (d, 2H), 7.42 (d, 2H), 6.43 (d, 2H), 3.98 (s, 1H), 3.88 (s, 1H), 2.54–2.34 (d, 6H). ^{13}C-NMR (d_6-DMSO) 178.04–42.24 (42 C). FAB-MS (mNBA): 856 $[Ru(phen)_2(4\text{-}N(CH_3)_2\text{-DPC})]^{2+}(Cl_2)^-$; 785 $[Ru(phen)_2(4\text{-}N(CH_3)_2\text{-DPC})]^{2+}$; 461 $[Ru(phen)_2]$; 324 [4-$N(CH_3)_2$-DPC].

2.4.6. $[Ru(bpy)_2(4\text{-}N(CH_3)_2\text{-DPC})]Cl_2$. 44%, black crystals, IR (KBr) cm^{-1}: 3467 (NH_2), 3044 (C–H), 2929 (C–H), 1682 (C=O), 1331 (C=S). Calcd for $C_{38}H_{36}Cl_2N_8Ru_1S_1$: C, 56.43; H, 4.49; N, 13.85. Found: C, 56.38; H, 4.37; N, 13.72%. ^{1}H NMR (DMSO-d_6): δ ppm: 8.98 (s, 1H), 8.64 (s, 1H), 8.40 (d, J = 4.9 Hz, 2H), 8.28 (d, J = 8.4 Hz, 2H), 8.08 (s, 1H), 7.85 (d, 2H), 7.58 (d, J = 5.0 Hz, 2H), 7.36 (m, 3H), 7.22 (d, 2H), 7.16 (d, 2H), 6.98 (d, 2H), 6.72 (d, J = 14.6 Hz, 2H), 6.64 (d, 2H), 6.36 (d, 2H), 6.28 (d, 2H), 4.01 (s, 1H), 3.96 (s, 1H), 2.68–2.32 (d, 6H). ^{13}C-NMR (d_6-DMSO) 177.84–41.44 (38 C). FAB-MS (m-NBA): 808 $[Ru(bpy)_2(4\text{-}N(CH_3)_2\text{-DPC})]^{2+}(Cl_2)^-$; 727 $[Ru(bpy)_2(4\text{-}N(CH_3)_2\text{-DPC})]^{2+}$; 413 $[Ru(bpy)_2]$; 324 [4-$N(CH_3)_2$-DPC].

2.4.7. [Ru(phen)$_2$(4-NO$_2$–DPC)]Cl$_2$. 46%, black crystals, IR (KBr) cm^{-1}: 3426 (NH_2), 3038 (C–H), 1339 (C=S). Calcd for $C_{40}H_{30}Cl_2N_8O_2Ru_1S_1$: C, 55.94; H, 3.52; N, 13.05. Found: C, 55.88; H, 3.48; N, 13.02%. ^{1}H NMR (DMSO-d$_6$): δ ppm: 8.86 (s, 1H), 8.83 (s, 1H), 8.80 (s, J = 4.9 Hz, 1H), 8.56 (d, J = 8.4 Hz, 2H), 8.38 (d, 2H), 8.06 (d, 2H), 7.94 (d, J = 5.0 Hz, 2H), 7.86 (d, 2H), 7.58 (d, 2H), 7.46 (d, 3H), 7.32 (d, 2H), 7.28 (d, J = 14.6 Hz, 2H), 7.25 (d, 2H), 7.18 (d, 2H), 6.25 (d, 2H), 3.86 (s, 1H), 3.82 (s, 1H). ^{13}C-NMR (d$_6$-DMSO) 174.26–116.28 (40 C). FAB-MS (mNBA): 858 [Ru(phen)$_2$(4-NO$_2$-DPC)]$^{2+}$(Cl$_2$)$^-$; 787 [Ru(phen)$_2$(4-NO$_2$-DPC)]$^{2+}$; 461 [Ru(phen)$_2$]; 326 [4-NO$_2$-DPC].

2.4.8. [Ru(bpy)$_2$(4-NO$_2$–DPC)]Cl$_2$. 43%, black crystals, IR (KBr) cm^{-1}: 3452 (NH_2), 3065 (C–H), 1328 (C=S). Calcd for $C_{36}H_{30}Cl_2N_8O_2Ru_1S_1$: C, 53.33; H, 3.73; N, 13.82. Found: C, 53.29; H, 3.66; N, 13.78%. ^{1}H NMR (DMSO-d$_6$): δ ppm: 8.76 (s, 1H), 8.72 (s, 1H), 8.62 (s, J = 4.9 Hz, 1H), 8.44 (d, J = 8.4 Hz, 2H), 8.26 (s, 1H), 8.24–8.18 (d, 2H), 8.04 (d, J = 5.0 Hz, 2H), 7.84 (d, 2H), 7.61 (d, 2H), 7.36 (d, 2H), 7.08 (d, 2H), 6.92 (d, J = 14.6 Hz, 2H), 6.88 (m, 4H), 6.56 (d, 2H), 6.17 (d, 2H), 3.23 (s, 1H), 3.12 (s, 1H). ^{13}C-NMR (d$_6$-DMSO) 169.42–121.64 (36 C). FAB-MS (mNBA): 810 [Ru(bpy)$_2$(4-NO$_2$-DPC)]$^{2+}$(Cl$_2$)$^-$; 729 [Ru(bpy)$_2$(4-NO$_2$-DPC)]$^{2+}$; 413 [Ru(bpy)$_2$]; 326 [4-NO$_2$-DPC].

2.4.9. [Ru(phen)$_2$(N-BITSZ)]Cl$_2$. 46%, black crystals, IR (KBr) cm^{-1}: 3445–3282 (NH_2 & N–H), 3062 (C–H), 2957 (C–H), 1682 (C=O), 1381 (C==S). Calcd for $C_{40}H_{30}Cl_2N_8O_1Ru_1S_1$: C, 57.01; H, 3.59; N, 13.30. Found: C, 56.98; H, 3.42; N, 13.22%. ^{1}H NMR (DMSO-d$_6$): δ ppm: 10.13 (d, J = 5.2 Hz, 1H), 9.11 (s, 1H, CH=N), 8.84 (d, J = 8.8 Hz, 2H), 8.66 (m, J = 8.6 Hz, 4H), 8.54 (d, J = 8.6 Hz, 2H), 8.47–8.21 (m, 6H), 8.10–8.01 (m, 2H), 7.81 (d, J = 5.0 Hz, 2H), 7.62–7.44 (m, 4H), 7.39 (m, 4H), 6.84 (s, 2H, br, NH_2). ^{13}C-NMR (d$_6$-DMSO) 180.48–46.84 (40 C). FAB-MS (mNBA): 842 [Ru(phen)$_2$(N-BITSZ)]$^{2+}$(Cl$_2$)$^-$; 772 [Ru(phen)$_2$(N-BITSZ)]$^{2+}$; 461 [Ru(phen)$_2$]; 381 [N-BITSZ].

2.4.10. [Ru(bpy)$_2$(N-BITSZ)]Cl$_2$. 43%, black crystals, IR (KBr) cm^{-1}: 3488–3385 (NH_2 & N–H), 3056 (C–H), 2968 (C–H), 1682 (C=O), 1361 (C==S). Calcd for $C_{36}H_{30}Cl_2N_8O_1Ru_1S_1$: C, 54.41; H, 3.80; N, 14.10. Found: C, 54.34; H, 3.79; N, 14.04%. ^{1}H NMR (DMSO-d$_6$): δ ppm: 10.05 (d, J = 5.2 Hz, 1H), 9.18 (s, 1H, CH=N), 8.76 (d, J = 8.8 Hz, 2H), 8.62 (d, J = 8.6 Hz, 2H), 8.51 (d, J = 8.6 Hz, 2H), 8.39–8.22 (m, 6H), 8.20–8.03 (m, 2H), 7.86 (d, J = 5.0 Hz, 2H), 7.64–7.45 (m, 4H), 7.28 (m, 4H), 6.54 (s, 2H, br, NH_2), 6.34 (d, 2H). ^{13}C-NMR (d$_6$-DMSO) 182.22–44.84 (36 C). FAB-MS (mNBA): 794 [Ru(bpy)$_2$(N-BITSZ)]$^{2+}$(Cl$_2$)$^-$; 723 [Ru(bpy)$_2$(N-BITSZ)]$^{2+}$; 413 [Ru(bpy)$_2$]; 381 [N-BITSZ].

2.4.11. [Ru(phen)$_2$(PTSZ)]Cl$_2$. 43%, black crystals, IR (KBr) cm^{-1}: 3450–3292 (NH_2 & N–H), 3060 (C–H), 2965 (C–H), 1630 (NH), 1328 (C==S). Calcd for $C_{30}H_{24}Cl_2N_8Ru_1S_1$: C, 51.43; H, 3.45; N, 15.99. Found: C, 51.38; H, 3.39; N, 15.92%. ^{1}H NMR (DMSO-d$_6$): δ ppm: 8.71 (s, J = 5.2 Hz, 1H), 8.62 (s, 1H, CH = N), 8.57 (d, J = 8.8 Hz, 2H), 8.34 (d, J = 8.6 Hz, 1H), 8.26 (d, J = 8.6 Hz, 1H), 7.95 (m, 3H), 7.86 (m, 2H), 7.63 (d, J = 5.0 Hz, 2H), 7.58 (d, 2H), 7.46 (d, 2H), 7.31 (s, 2H, br, NH_2), 6.86

(d, 2H), 3.81 (d, 2H), 2.21 (s, 1H). ^{13}C-NMR (d_6-DMSO) 184.86–106.62 (30 C). FAB-MS (mNBA): 700 $[Ru(phen)_2(PTSZ)]^{2+}(Cl_2)^-$; 629 $[Ru(phen)_2(PTSZ)]^{2+}$; 461 $[Ru(phen)_2]$; 168 [PTSZ].

2.4.12. [Ru(bpy)$_2$(PTSZ)]Cl$_2$. 43%, black crystals, IR (KBr) cm^{-1}: 3441–3278 (NH_2 & N–H), 3148 (C–H), 2980 (C–H), 1670 (NH), 1349 (C=S). Calcd for $C_{26}H_{24}Cl_2N_8Ru_1S_1$: C, 47.85; H, 3.71; N, 17.17. Found: C, 47.74; H, 3.69; N, 17.12%. ^{1}H NMR (DMSO-d_6): δ ppm: 8.75 (s, J = 5.2 Hz, 1H), 8.64 (s, 1H, CH=N), 8.61 (d, J = 8.8 Hz, 2H), 8.56 (d, J = 8.6 Hz, 1H), 8.47 (d, J = 8.6 Hz, 1H), 8.36 (m, 3H), 8.24 (s, 1H), 7.98 (d, J = 5.0 Hz, 2H), 7.88 (d, 2H), 7.62 (d, 1H), 7.34 (s, 2H, br, NH_2), 7.22 (d, 2H), 6.75 (d, 2H), 3.98 (d, 2H), 2.06 (s, 1H). ^{13}C-NMR (d_6-DMSO) 181.28–112.40 (26 C). FAB-MS (mNBA): 652 $[Ru(bpy)_2(PTSZ)]^{2+}(Cl_2)^-$; 581 $[Ru(bpy)_2(PTSZ)]^{2+}$; 413 $[Ru(bpy)_2]$; 168 [PTSZ].

2.4.13. [Ru(phen)$_2$(PINH)]Cl$_2$. 43%, black crystals, IR (KBr) cm^{-1}: 3320 (N–H), 3120 (C–H), 2943 (C–H), 1648 (C==O). Calcd for $C_{35}H_{26}Cl_2N_8O_1Ru_1S_1$: C, 56.30; H, 3.51; N, 15.01. Found: C, 56.18; H, 3.49; N, 14.96%. ^{1}H NMR (DMSO-d_6): δ ppm: 8.82 (d, J = 5.2 Hz, 1H), 8.80 (s, 1H, CH=N), 8.64 (d, J = 8.8 Hz, 2H), 8.51 (d, J = 8.6 Hz, 1H), 8.41 (d, J = 8.6 Hz, 1H), 8.23 (s, 1H), 7.93 (m, 2H), 7.81 (d, J = 5.0 Hz, 2H), 7.74–7.58 (m, 4H), 7.49 (d, 2H), 7.02 (s, 1H), 6.80 (s, 2H, br, NH_2), 6.65 (d, 2H), 5.68 (s, 1H), 5.65 (d, 2H), 2.08 (s, 1H). ^{13}C-NMR (d_6-DMSO) 166.04–104.26 (35 C). FAB-MS (mNBA): 746 $[Ru(phen)_2(PINH)]^{2+}(Cl_2)^-$; 675 $[Ru(phen)_2(PINH)]^{2+}$; 461 $[Ru(phen)_2]$; 214 [PINH].

2.4.14. [Ru(bpy)$_2$(PINH)]Cl$_2$. 43%, black crystals, IR (KBr) cm^{-1}: 3242 (N–H), 3164 (C–H), 2980 (C–H), 1652 (C==O). Calcd for $C_{31}H_{26}Cl_2N_8O_1Ru_1S_1$: C, 53.30; H, 3.75; N, 16.04. Found: C, 53.28; H, 3.69; N, 15.99%. ^{1}H NMR (DMSO-d_6): δ ppm: 8.93 (d, J = 5.2 Hz, 2H), 8.64 (s, 1H, CH=N), 8.58 (s, J = 8.8 Hz, 1H), 8.21 (d, J = 8.6 Hz, 1H), 7.70–7.62 (m, J = 8.6 Hz, 3H), 7.42–7.31 (m, 4H), 6.78 (m, 2H), 6.61 (d, J = 5.0 Hz, 2H), 6.58–6.28 (m, 4H), 6.18 (d, 2H), 5.61 (s, 2H), 5.54 (s, 1H) 2.01 (s, 1H). ^{13}C-NMR (d_6-DMSO) 162.46–108.28 (31 C). FAB-MS (mNBA): 698 $[Ru(bpy)_2(PINH)]^{2+}(Cl_2)^-$; 627 $[Ru(bpy)_2(PINH)]^{2+}$; 413 $[Ru(bpy)_2]$; 214 [PINH].

3. Results and discussion

3.1. *Chemistry*

The ligands like 3-phenyl-5-(3,4,5,-tri-OCH_3-phenyl)-4,5-dihydro 1*H*-pyrazole-1-carbothioamide were prepared by reacting 3,4,5-tri-methoxy benzylidene chalcone with appropriate thiosemicarbazide in alcohol at 1 : 1 M ratio, ligands like 3-phenyl-5-(p-tolyl)-4,5-dihydro 1*H*-pyrazole-1-carbothioamide were prepared by reacting 4-methyl benzylidene chalcone with appropriate thiosemicarbazide in alcohol at 1 : 1 M ratio. Ligands like PTSZ and PINH were prepared by reacting pyrrole-2-carbaldehyde with thiosemicarbazide and isoniazide in alcohol at 1 : 1 M ratio. N-BITSZ was prepared by reacting N-benzyl isatin with thiosemicarbazide in alcohol at 1 : 1 M ratio (schemes 1–3). Structures of the

synthesized ligands and complexes were established by UV–vis, FT-IR, ^{1}H-NMR, ^{13}C-NMR, elemental analysis and mass spectral analysis (Supplementary material).

3.1.1. UV spectra. The ruthenium complexes showed broad and intense visible bands 320–530 nm due to metal to ligand charge transfer transition (MLCT). In the UV region, bands at 270 and 300 nm were assigned to 2,2′-bipyridine/1,10-phenanthroline π–π∗ transitions, found in free 2,2′-bipyridine/1,10-phenanthroline at 270 nm, so that coordination resulted in a red shift in the transition energy. There were also two shoulders at 380 and 500 nm, which were, tentatively, attributed to MLCTs involving 2,2′-bipyridine, 1,10-phenanthroline, and the third ligand (schemes 4 and 5).

3.1.2. IR spectra. In the phenyl pyrazoline ligands, absorptions from 3500–3400 for NH_2, 3150–3000 cm^{-1} for C–H aromatic stretching, 2980–2850 cm^{-1} for C–H aliphatic stretching, and 1585–1500 cm^{-1} for C=N stretching, 1380–1320 cm^{-1} for C=S stretching were observed. Pyrrole thiosemicarbazone ligands showed absorptions from 3410–3200 cm^{-1} for NH_2 and NH stretching, from 3150–3000 cm^{-1} for C–H aromatic stretching, and from 1370–1320 cm^{-1} for C=S stretching. In pyrrole isonicotinylhydrazones, absorptions from 3300–3200 for NH stretching, 3150–3000 cm^{-1} for C–H aromatic stretching, and 1680–1620 cm^{-1} for C=O stretching were observed. R_f value of all the ligands were determined.

$Ru(phen)_2(3,4,5\text{-tri-}OCH_3\text{-DPC})]Cl_2$ has bands at 3483 for NH_2, 3040 for CH and 1324 for C=S, whereas 3,4,5-tri-OCH_3-DPC they are at 3480 for NH_2, 3042 for C–H and 1346 for C=S. By comparison of IR spectra of complexes with pyrazolines coordination occurs

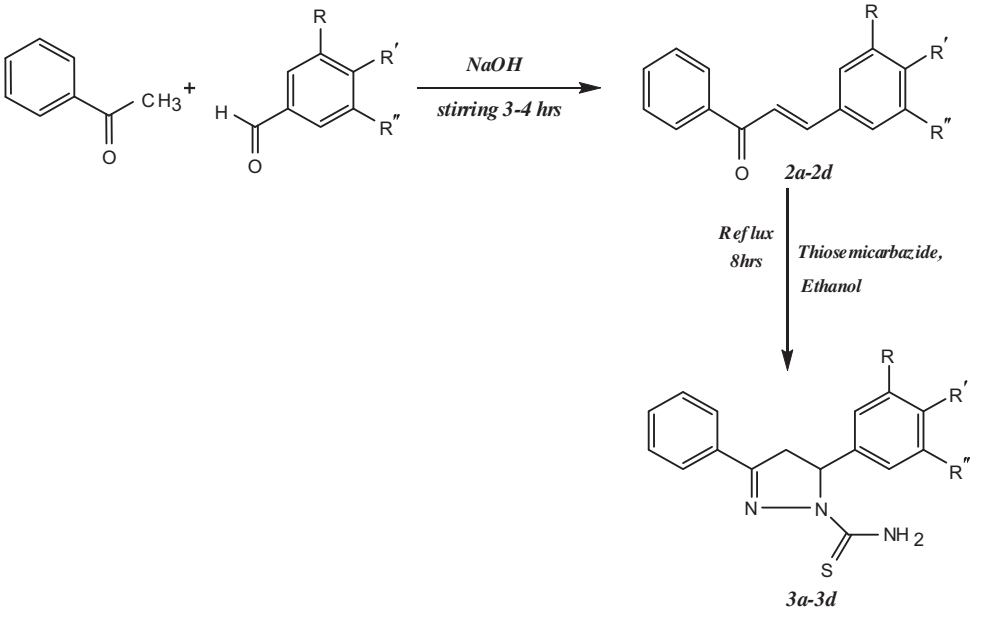

Scheme 1. Preparation of pyrazole ligands. **2a**, R = OCH_3, R′ = OCH_3, R″ = OCH_3; **2b**, R = H, R′ = CH_3, R″ = H; **2c**, R = H, R′ = $N(CH_3)_2$, R″ = H; **2d**, R = H, R′ = NO_2, R″ = H. **3a**, R = OCH_3, R′ = OCH_3, R″ = OCH_3; **3b**, R = H, R′ = CH_3, R″ = H; **3c**, R = H, R′ = $N(CH_3)_2$, R″ = H; **3d**, R = H, R′ = NO_2, R″ = H.

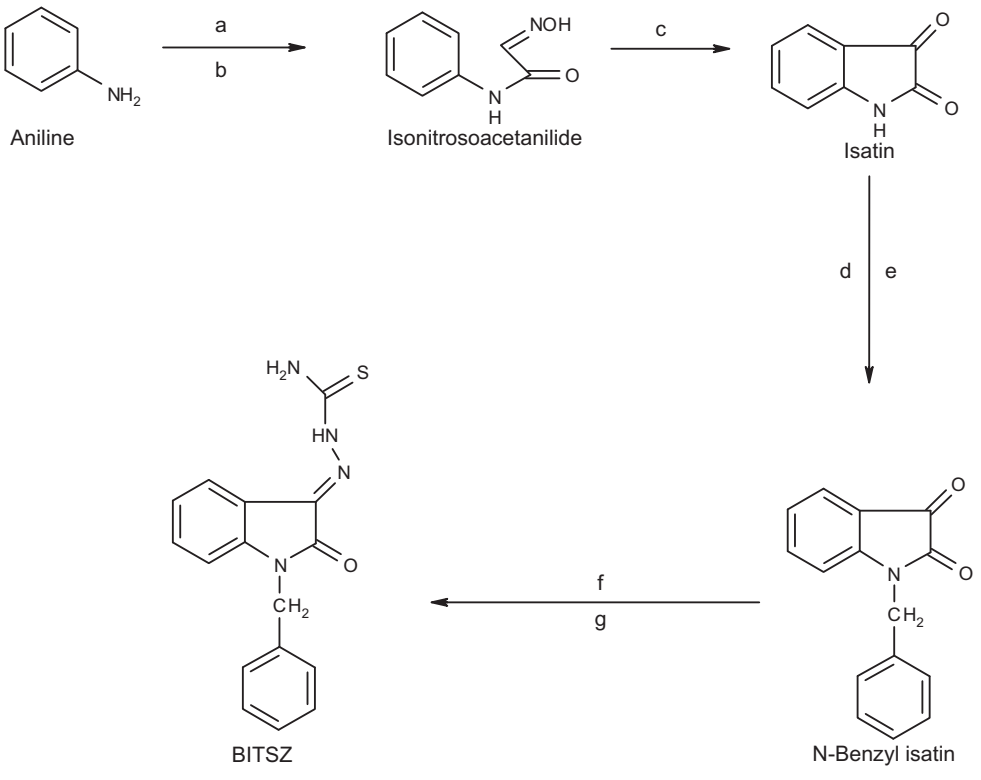

Scheme 2. Preparation of N-benzyl isatin thiosemicarbazone [35, 36]. Reagents (a) $Cl_3CCH(OH)_2$; (b) NH_2OH. HCl; (c) H_2SO_4; (d) DMF/K_2CO_3; (e) C_6H_5–CH_2Cl; (f) $NH_2NHCSNH_2$; (g) Alcohol, CH_3COOH.

by sulfur and nitrogen (Supplementary figures 1–18). In the complexes with pyrrole thiosemicarbazones, spectra confirm coordination by sulfur and imino nitrogen. In pyrrole isonicotinyl hydrazone complexes, coordination by oxygen and imino nitrogen was confirmed by the spectra. These compounds do not possess C2 axes of symmetry. Such a loss of C2 axis of symmetry was seen for $[Ru(L)_2(R)]$ [37] (where L = 2,2′-bipyridine/1,10-phenanthroline and R = acetazolamide, 7-iodo-8-hydroxy-quinoline, etc.). All compounds had well-resolved resonances, which correspond to four different aromatic ring protons of the two 2,2′-bipyridine/1,10-phenanthroline ligands and third ligand.

3.1.3. ^{1}H-NMR spectra. In ^{1}H-NMR spectra of the 3-phenyl-5-(3,4,5-tri-OCH_3-phenyl)-4,5-dihydro 1*H*-pyrazole-1-carbothioamide, there were 12 resolved resonances at δ 8.05–5.86 and nine resolved resonances at δ 3.86–3.79 due to 3 OCH_3 groups.

In ^{1}H-NMR spectra of $[Ru(bpy)_2(3,4,5\text{-tri-}OCH_3\text{-DPC})]Cl_2$, there were 28 resonances (δ 8.26–5.9) and nine resolved resonances at δ 3.91–3.80 due to 3 OCH_3 groups. ^{1}H-NMR of the complexes having more protons confirmed the authenticity of complex.

In ^{1}H-NMR spectra of the complexes, there were resolved resonances at δ 10.13. Thus, for $[Ru(phen)_2(N\text{-BITSZ})]Cl_2$, there were 30 resonances (δ 10.13–6.84) and 30 well-resolved peaks (δ 10.05–6.54) for $[Ru(bpy)_2(N\text{-BITSZ})]Cl_2$.

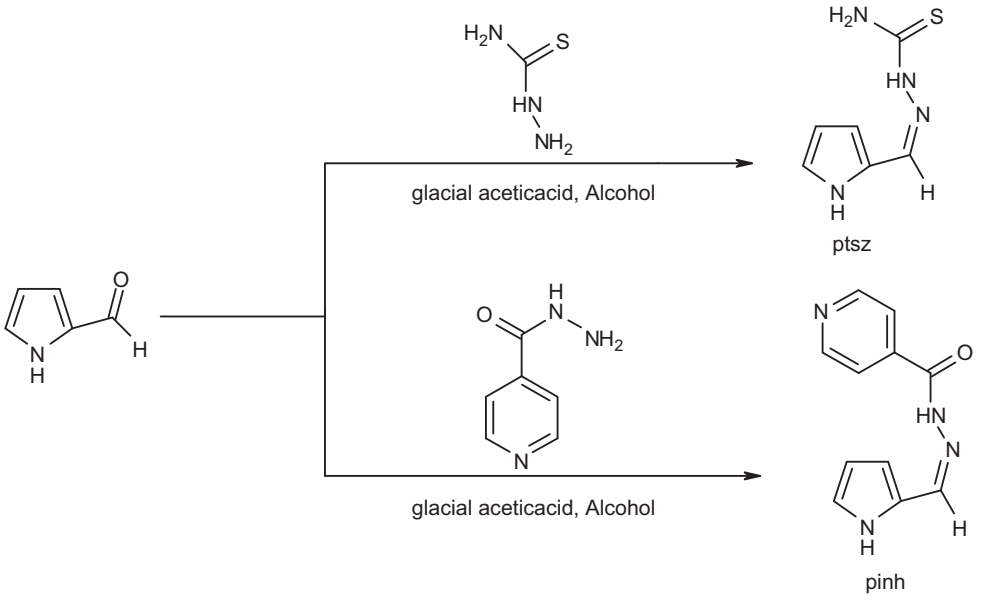

Scheme 3. Preparation of ptsz and pinh [38].

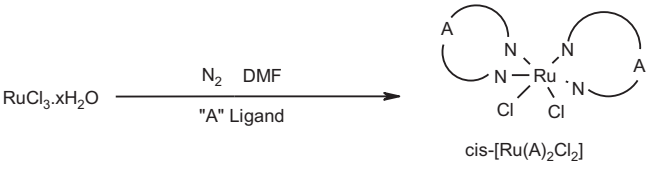

Scheme 4. Preparation of *cis*-$[Ru(A)_2Cl_2]$.

3.1.4. Mass spectra. Spectra showed numerous peaks representing successive degradation of the molecules. FAB mass spectroscopic data in Supplementary Figure 15 clearly suggest that mononuclear complexes formed in each case, the first fragment being due to $[Ru(A)_2(B)]^{2+}$ Cl_2^- ion pair. The complex also showed a peak due to the complex cation $[Ru(A)_2(B)]^{2+}$ and others due to $[Ru(A)(B)]^{2+}$, $[Ru(A)_2]^{2+}$, respectively (where A = 1,10-phenanthroline/2,2′-bipyridine and B = 3,4,5-tri-OCH_3-DPC, 4-CH_3-DPC, 4-N-$(CH_3)_2$-DPC, 4-NO_2-DPC, N-BITSZ, PTSZ and PINH]. This type of fragmentation was reported for $[Ru(phen)_2(nmit)]Cl_2$ and $[Ru(bpy)_2(ihqs)]Cl_2$, where nmit = N-methyl isatin thiosemicarbazone and ihqs = 7-iodo-8-hydroxy quinoline-5-sulfonic acid [45]. Loss of chloride was detected where A = 2,2′-bipyridine/1,10-phenanthroline and B = r-DPC, PTSZ, PINH. Thus, based on the above observations, it is tentatively suggested that Ru(II) complexes have pseudooctahedral geometry.

3.2. *Biological activity and discussion*

The *in vitro* cytotoxic activity was evaluated for ligands and complexes against human 4/C8, CEM, T-lymphocytes as well murine L1210 cells, HL-60, and BEL-7402; results are

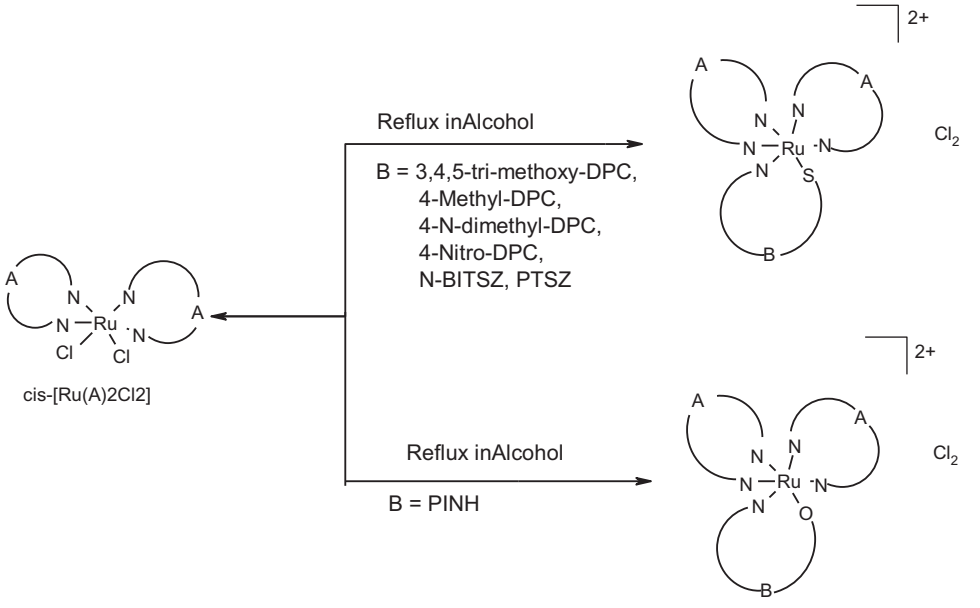

Scheme 5. Preparation of tris chelates from *cis*-$[Ru(A)_2Cl_2]$.

Table 1. Cytotoxic studies of ligands.

	IC_{50}[a] (μM)				
Compound	CEM	L1210	Molt 4/C8	HL60	BEL7402
3,4,5-tri-OCH_3-DPC	54 ± 08	28 ± 04	88 ± 16	58 ± 02	66 ± 04
4-CH_3-DPC	86 ± 14	98 ± 12	42 ± 08	82 ± 08	50 ± 02
N-$(CH_3)^2$-DPC	48 ± 06	44 ± 08	104 ± 18	54 ± 06	92 ± 14
4-NO_2-DPC	106 ± 04	116 ± 12	134 ± 12	231 ± 08	225 ± 12
N-BITSZ	128 ± 16	122 ± 14	68 ± 16	118 ± 04	104 ± 08
PTSZ	84 ± 22	96 ± 14	48 ± 14	42 ± 08	96 ± 06
PINH	158 ± 18	184 ± 06	78 ± 12	144 ± 14	100 ± 14

summarized in tables 1 and 2. The relative potencies between ligands and their ruthenium complexes revealed the importance of ruthenium using the Molt $4/C_8$, CEM, assays and murine L1210 assays. These determinations showed that ruthenium complexes were more potent.

Results are summarized in table 2 for 14 complexes tested for *in vitro* cytotoxic activity against human cancer cell lines CEM, L1210, Molt 4/C8, HL60, Molt 4/C8, and murine tumor cell line, BEL7402. Cells were seeded in 200 l-micro titer plate wells in RPMI-1640 culture medium (supplemented with fetal calf serum (10%), 2 Mm L-glutamine and 0.075% $NaHCO_3$) in the absence or presence of test compounds (200, 40, 8, 1.6 and 0.32 μg/mL). The cell number was counted after two (L1210) or three (CEM, Molt4) days using a Coulter counter.

In vitro evaluation of these ruthenium complexes revealed cytotoxic activities from 0.24 to >2 μM against CEM, 0.28 to >2 μM against L1210, 0.36 to >2 μM against Molt4/C8, 0.24 to >2 μM against HL60 and 0.25 to >2 μM against BEL7402. Of the tested ruthenium

Table 2. Cytotoxic studies of ruthenium complexes.

	IC_{50}[a] (μM)				
Comp. code	CEM	L1210	Molt 4/C8	HL60	BEL7402
R-1	0.75 ± 0.06	0.28 ± 0.04	0.95 ± 0.3	0.24 ± 0.02	0.58 ± 0.06
R-2	1.1 ± 0.4	0.99 ± 0.2	1.7 ± 0.5	0.58 ± 0.04	0.36 ± 0.04
R-3	0.24 ± 0.03	0.35 ± 0.02	0.57 ± 0.05	0.34 ± 0.04	0.84 ± 0.06
R-4	0.71 ± 0.05	0.49 ± 0.03	0.44 ± 0.04	0.63 ± 0.07	0.92 ± 0.08
R-5	0.54 ± 0.05	0.59 ± 0.04	0.86 ± 0.06	0.28 ± 0.04	0.44 ± 0.06
R-6	0.97 ± 0.2	1.5 ± 0.3	0.94 ± 0.3	0.45 ± 0.05	0.25 ± 0.03
R-7	1.4 ± 0.4	1.2 ± 0.2	1.9 ± 0.7	0.94 ± 0.06	1.2 ± 0.4
R-8	0.88 ± 0.1	0.42 ± 0.03	0.62 ± 0.05	0.58 ± 0.04	0.64 ± 0.06
R-9	0.47 ± 0.04	0.98 ± 0.3	0.36 ± 0.04	0.44 ± 0.04	0.46 ± 0.02
R-10	0.68 ± 0.05	0.46 ± 0.04	0.77 ± 0.03	0.30 ± 0.02	0.51 ± 0.03
R-11	1.2 ± 0.07	1.8 ± 0.2	0.98 ± 0.04	1.0 ± 0.4	1.6 ± 0.06
R-12	2.4 ± 0.08	1.4 ± 0.04	2.9 ± 0.5	3.2 ± 0.06	1.2 ± 0.6
R-13	1.6 ± 0.04	0.92 ± 0.2	1.1 ± 003	1.4 ± 0.06	2.4 ± 0.04
R-14	3.4 ± 0.08	2.2 ± 0.02	2.8 ± 0.06	1.9 ± 0.05	1.8 ± 0.02
STD	0.51 ± 0.1	1.2 ± 0.02	0.87 ± 0.06	0.98 ± 0.02	0.78 ± 0.04

[a]50% inhibitory concentration, required to inhibit tumor cell proliferation by 50%.

complexes, R-3 shows potent cytotoxic activity against the entire five cell lines tested, 0.24, 0.35, 0.57, 0.34, and 0.84 μM for CEM, L1210, Molt4/C8, HL60, BEL7402, respectively. R-5 shows significant cytotoxic activity against the entire five cell lines of 0.54, 0.59, 0.86, 0.28, 0.44 μM for CEM, L1210, Molt4/C8, HL60, BEL7402, respectively.

The remaining ruthenium complexes showed low μM values for Molt 4, HL60, and CEM and higher μM values for L1210 and BEL7402. Some ruthenium complexes showed low μM values for L1210, BEL7402, and CEM and higher μM values for Molt 4 and HL60.

In comparison with ruthenium compounds, the ligands displayed cytotoxicities at higher concentration. Thus, the ruthenium compounds proved inhibitory to tumor growth at submicromolar concentration where the ligands were not antitumorally active.

All of these Ru(II) complexes can bind to DNA through intercalation with high DNA-binding affinities and also possess DNA-cleaving capacity. At 50 and 100 μM, almost complete DNA unwinding can be observed.

3.3. *DNA-binding and DNA-unwinding properties*

The electronic spectra of all these Ru(II) compounds in water (0.1% DMSO) are characterized by an intense MLCT in the visible region [2]. Visible bands around 450 nm arise from metal to ligand (π) charge transfer transitions. UV–Visible spectra showed that all of these ruthenium complexes exhibit hypochromism accompanied by bathochromic shifts upon addition of CT-DNA.

3.3.1. Electronic absorption titration. Absorption titrations of Ru(II) complexes in buffer A were performed by using a fixed Ru(II) concentration to which increments of DNA stock solutions were added. Initially, 3000 μL solutions of the blank buffer solution and the Ru(II) complex were placed in the reference and sample cuvettes (1 cm path length), respectively, and then, the first spectrum was recorded from 200 to 640 nm. During the

titration, an aliquot (3–10 μL) of DNA stock solution was added to each cuvette to eliminate the absorbance of the DNA itself, and the solutions were mixed by repeated inversion. The solutions were allowed to incubate for 5 min before absorption spectra were recorded. The titration processes were repeated until there was no change in the spectra for at least 4 titrations, indicating binding saturation. The changes in Ru(II) complex concentration due to dilution at the end of each titration were negligible. The intrinsic binding constants of both complexes, Kb to DNA were obtained by monitoring the changes of the MLCT absorbance for both complexes according to equations (1) and (2) [39–42]

$$[(\varepsilon_a - \varepsilon_f)/(\varepsilon_b - \varepsilon_f) = (b - (b^2 - 2K_b^2 C_t[DNA]/S)^{1/2}]2K_b C_t \quad (1)$$

$$b = 1 + K_b C_t + K_b[DNA]/2s \quad (2)$$

where ε_a is the extinction coefficient (A_{abs}/[M]) observed for the MLCT absorption band at a given DNA concentration, ε_f and ε_b the extinction coefficient for the free Ru(II) complex and the extinction coefficient for the Ru(II) complex in the fully bound form, respectively, the concentration of DNA in nucleotides, C_t the total Ru(II) complex concentration, K_b the equilibrium binding constant (in $M\,L^{-1})^{-1}$, and s the binding site size.

3.4. *Structure–activity relationships and antitumor mechanism*

DNA is the main target of antitumor activity in most antitumor compounds [39]. The heavy metal complexes can be designed to target particular sequences or structural features of the DNA double helix with binding greatly influenced by the structure of DNA [40]. Many antiviral, antitumor and antibacterial agents take action through binding to DNA. The binding of these drugs can be attributed to electrostatic forces, hydrophobic interaction, hydrogen bonds, etc. The DNA binding constants (K_b) are rather high (0.31–$1.49 \times 10^5\,m^{-1}$). These complexes also possess good DNA-cleaving ability. The most important phenomena for complexes showing antitumor activity is interaction between the complexes and DNA by intercalation.

In cancer chemotherapy, DNA-targeting agents play an important role [41], such as cisplatin, [*cis*-($PtCl_2(NH_3)_2$], carboplatin ([Pt(CBDCA)-$(NH_3)_2$], CBDCA = 1,1-cyclobutane dicarboxylato), and oxoplatin ([Pt(dach)(oxaloto)] dach = R,R-1,2-diamino cyclohexane). All these structures have the general structure of *cis*-[PtX_2(amine)$_2$], where X is a leaving group such as chloride or dicarboxylate. All of the Ru(II) complexes are different from cisplatin, coordination-saturated with no leaving group. The most important structural feature is they contain aromatic and heterocyclic (pyrazole) moieties and all of them can bind to DNA. Most of the Ru(II) complexes show strong DNA-binding affinities and they can easily interact with the DNA of tumor cells.

In our research, it is found that all these synthesized complexes possess excellent antitumor activities, whereas their corresponding ligands do not, which is closely correlated with the structural (N,S,O) characteristics (including the electronic structure) of these Ru(II) bipyridyl and phenanthroline complexes. The mononuclear Ru(II) complexes (Ru(phen)$_2$L)$^{2+}$ adopt pseudooctahedral geometry with an N-, S-, and O-containing heterocyclic ligand as an intercalative ligand (L) of the complex. Free ligands have the same planarity and can intercalate between DNA-base pairs. Energies of the lowest unoccupied molecular orbitals (LUMO and LUMO + x), which usually accept the electron offered from

DNA-base pairs, are different [42, 43]. The Ru^{+2} introduces high-positive charge making the energies of the frontier molecular orbital (LUMO) reduced. The comparisons of some frontier molecular orbital energies between the complexes and corresponding ligands are given in Supplementary material.

Some of the complexes possess the most potent anticancer activity, although their DNA-binding affinities are not strongest in this series of complexes. The energy difference ($\Delta E_L - H$) and the hydrophobic parameters usually expressed as logP of the complexes may be important. Quantitative–structure–activity relationships for pharmaceutical compounds have shown that the anticancer activity (PIc_{50}) of ruthenium complexes is closely related to logp [44]. In our research, the dipole moments of the complexes can be obtained with DFT calculations and used to quantitatively analyze the trend in the hydrophobic values (logP), although logP data cannot be experimentally measured. The complexes have poor water solubility; according to the similarity theorem, it means that they have rather good fat solubility. Since most antimetastatic agents perform their activity in organic solvents, this may be one reason why the complexes possess higher anticancer activity. From the table, the energy differences ($\Delta E_L - H$) of the ruthenium complexes 5 and 6 are greater than can be reasonably explained.

In some of the heterocyclic ligands, substitution of the p-site on the intercalative ligand seems to be more advantageous than that of the o-site. It may be related to atomic net charge population on the intercalative ligand. Substitution of the p-site provides more balanced polarity alteration of the charge populations on the intercalative ligand than that of the o-site; research on QSAR is underway.

4. Conclusion

The *in vitro* anticancer activities of a series of Ru(II) polypyridine complexes $[Ru(A)_2(B)]^{2+}$, where A = 2,2′-bipyridine/1,10-phenanthroline and B = 3,4,5-tri-OCH_3-DPC, 4-CH_3-DPC, 4-$N(CH_3)_2$-DPC, 4-NO_2-DPC, N-BITSZ, PTSZ, PINH and their corresponding ligands have been measured against human cancer T-lymphocyte cell lines molt 4/c8 and CEM, murine tumor leukemia cell line L1210, human promyelocytic leukemia cells (HL-60) and Bel-7402 liver cancer cells by MTT assay. These ruthenium complexes possess excellent *in vitro* cytotoxic activities; the corresponding ligands are not as cytotoxic. The relationship between anticancer potency and the DNA-binding affinity was analyzed to get possible QSAR, but the anticancer efficiency is not in line with DNA-binding affinity. The complexes show good binding to calf thymus DNA and most exhibit efficient DNA cleavage upon irradiation via a mechanistic pathway involving formation of singlet oxygen as the reactive species. These results suggest that both ancillary ligand and intercalative ligand influence the binding of these complexes to DNA. In comparison with previously reported ruthenium complexes these new complexes show significant cytotoxic activities and DNA-binding constants [45–52].

Acknowledgement

One of the authors Mrs. Srujana Vallala is thanking the Department of Science & Technology (DST), New Delhi, India, for providing the funds for carrying research (SR/WOS-A/LS-562/2011) dated 27/03/2012.

References

[1] F. Wang, J. Xu, A. Habtemariam, J. Bella, P.J. Sadler. *J. Am. Chem. Soc.*, **127**, 17734 (2005).
[2] V.B. Arion, E. Reisner, M. Fremuth, M.A. Jakupec, B.K. Keppler, V.Y. Kukushkin, A.J.L. Pombeiro. *Inorg. Chem.*, **42**, 6024 (2003).
[3] E. Alessio. *Chem. Rev.*, **104**, 4203 (2004).
[4] U.K. Mazumder, M. Gupta, S.S. Karki, S. Bhattacharya, S. Rathinasamy, T. Sivakumar. *Bioorg. Med. Chem.*, **13**, 5766 (2005).
[5] C.G. Hartinger, A. Casini, C. Duhot, Y.O. Tsybin, L. Messori, P.J. Dyson. *J. Inorg. Biochem.*, **102**, 2136 (2008).
[6] C.S. Allardyce, P.J. Dyson, D.J. Ellis, P.A. Salter, R. Scopelliti. *J. Organomet. Chem.*, **668**, 35 (2003).
[7] W. Kondioller, C.G. Hartinger, A.A. Nazarov, J. Kasser, R. John, M.A. Jakupec, V.B. Arion, P.J. Dyson, B. K. Keppler. *J. Organomet. Chem.*, **694**, 922 (2009).
[8] C.A. Vock, W.H. Ang, C. Scolaro, A.D. Phillips, L. Lagopoulos, J. Juillerat-Jeanneret, G. Sava, R. Scopelliti, P.J. Dyson. *J. Med. Chem.*, **50**, 2166 (2007).
[9] M.J. Clarke, F. Zhu, D.R. Frasca. *Chem. Rev.*, **99**, 2511 (1999).
[10] I. Bratsos, B. Serli, E. Zangrando, N. Katsaros, E. Alessio. *Inorg. Chem.*, **46**, 975 (2007).
[11] C.S. Allardyce, A. Dorcier, C. Scolaro, P.J. Dyson. *Appl. Organomet. Chem.*, **19**, 1 (2005).
[12] C.X. Zhang, S.T. Lippard. *Curr. Opin. Chem. Biol.*, **7**, 481 (2003).
[13] S. Kapitza. *Dalton Trans.*, 4929 (2007).
[14] S. Kapitza, M. Pongratz, M.A. Jakupec, P. Heffeter, W. Berger, L. Lackinger, B.K. Keppler, B. Marian. *J. Cancer Res. Clin. Oncol.*, **131**, 101 (2005).
[15] H.L. Huang, Z.Z. Li, Z.H. Liang, J.H. Yao, Y.J. Liu. *Eur. J. Med. Chem.*, **46**, 3282 (2011).
[16] Y.J. Liu, C.H. Zeng, Z.H. Liang, J.H. Yao, H.L. Huang, Z.Z. Li, F.H. Wu. *Eur. J. Med. Chem.*, **45**, 3087 (2010).
[17] A.E. Eid. *Int. J. Chem.*, **1**, 1 (1999).
[18] Z.H. Chohan, H. Pervez, A. Rauf, A. Scozzafava, C.T. Supuran. *J. Enzyme Inhib. Med. Chem.*, **17**, 117 (2002).
[19] M. Sulu, H. Kucukbay, R. Durmaz, S. Gunal. *Microbiological.*, **23**, 73 (2000).
[20] Z.H. Chohan, H. Pervez, A. Rauf, A. Scozzafava, C.T. Supuran. *J. Enzyme Inhib. Med. Chem.*, **18**, 259 (2002).
[21] A. Martinez, J. Suarez, T. Shand, R.S. Magliozzo, R.A. Sanchez-Delgado. *J. Inorg. Biochem.*, **105**, 39 (2011).
[22] S. Thota, S.S. Karki, K.N. Jayaveera, J. Balzarini, E. De Clercq. *J. Enzyme Inhib. Med. Chem.*, **25**, 513 (2010).
[23] M. Cocchietto, G. Sava. *Pharmacol. Toxicol.*, **87**, 193 (2000).
[24] S. Zorzet, A. Sorc, C. Casarsa, M. Cocchietto, G. Sava. *Met. Based. Drugs*, **8**, 1 (2001).
[25] G. Sava, A. Bergamo. *Int. J. Oncol.*, **17**, 353 (2000).
[26] R. Gagliardi, G. Sava, S. Pacor, G. Mestroni, E. Alessio. *Clin. Exp. Metastasis*, **12**, 93 (1994).
[27] M. Maganarin, A. Bergamo, M.E. Carotenuto, S. Zorzet, G. Sava. *Anticancer Res.*, **20**, 2939 (2000).
[28] J.M. Rademaker-Lakhai, D. van den Bongard, D. Pluim, J.H. Beijnen, J.H.M. Schellens. *Clin. Cancer Res.*, **10**, 3717 (2004).
[29] A. Vessieres, S. Top, W. Beck, H. Chen, E. Hillard, G. Jaouen. *Dalton Trans.*, 529 (2006).
[30] G. Jaouen (Ed.). *Bioorganometallics*, Wiley-VCH, Weinheim (2005).
[31] R.E. Morris, R.E. Aird, P. del Socorro Murdoch, H. Chen, J. Cummings, N.D. Hughes, S. Parsons, A. Parkin, G. Boyd, D.I. Jodrell, P.J. Sadler. *J. Med. Chem.*, **44**, 3616 (2001).
[32] S.S. Karki, S. Thota, S.Y. Darj, J. Balzarini, E. De Clercq. *Bioorg. Med. Chem.*, **15**, 6632 (2007).
[33] M. Grazia Mamalo, D. Zampieri, V. Falagiani, L. Vio, E. Banfi. *IL Farmaco*, **56**, 593 (2001).
[34] G. Menozzi, L. Merello, P. Fossa, S. Schenone, A. Ranise, L. Mosti, F. Bondavalli, R. Loddo, C. Murgioni, V. Mascia, P. La Colla. *Bioorg. Med. Chem.*, **12**, 5465 (2004).
[35] F.A. Mohammed, E.S. Hassan. *Arch Pharmacol*, **3**, 604 (2003).
[36] I. Chiyanzu, E. Hansell, J. Gut, P.J. Rosenthal, J.H. McKerrow, K. Chibale. *Bioorg. Med. Chem. Lett.*, **13**, 3527 (2003).
[37] U.K. Mazumder, M. Gupta, S. Bhattacharya, S.S. Karki, S. Rathinasamy, S. Thangavel. *J. Enzyme Inhib. Med. Chem.*, **19**, 185 (2004).
[38] T. Aboul-Fadl, F.A. Mohammed, E.S. Hassan. *Arch Pharmacal. Res.*, **26**, 778 (2003).
[39] F. Gao, H. Chao, F. Zhou, Y.X. Yuan, B. Peng, L.N. Ji. *J. Inorg. Biochem.*, **100**, 1487 (2006).
[40] X.W. Liu, J. Li, H. Li, K.C. Zheng, H. Chao, L.N. Ji. *J. Inorg. Biochem.*, **99**, 2372 (2005).
[41] M.T. Carter, M. Rodriguez, A.J. Bard. *J. Am. Chem. Soc.*, **111**, 8901 (1989).
[42] J.A.R. Navarro, J.M. Salas, M.A. Romero, R. Vilaplana, F. Gonzalez-Vilchez, R. Faure. *J. Med. Chem.*, **41**, 332 (1998).
[43] A. Harris, Y. Qu, N. Farrell. *Inorg. Chem.*, **44**, 1196 (2005).
[44] M.E. Budiman, U. Bierbach, R.W. Alexander. *Biochemistry*, **44**, 11262 (2005).

[45] D. Reha, M. Kabelac, F. Ryjacek, J. Sponer, J.E. Sponer, M. Elstner, S. Suhai, P. Hobza. *J. Am. Chem. Soc.*, **124**, 3366 (2002).
[46] X. Yang, Y. Liu, S. Yao, Y. Xia, Q. Li, W. Zheng, L. Chen, J. Liu. *J. Coord. Chem.*, **64**, 1491 (2011).
[47] Z.H. Liang, Z.Z. Li, H.L. Huang, Y.J. Liu. *J. Coord. Chem.*, **64**, 3342 (2011).
[48] X.L. Hong, Z.H. Liang, M.H. Zeng. *J. Coord. Chem.*, **64**, 3792 (2011).
[49] X.W. Liu, L. Li, J.L. Lu, Y.D. Chen, D.S. Zhang. *J. Coord. Chem.*, **64**, 4344 (2011).
[50] L. Xu, N.J. Zhong, Y.Y. Xie, H.L. Huang, Z.H. Liang, Z.Z. Li, Y.J. Liu. *J. Coord. Chem.*, **65**, 55 (2012).
[51] A.A.G. Al Abdel Hamid, S. Kanan. *J. Coord. Chem.*, **65**, 420 (2012).
[52] C. Shobha Devi, S. Satyanarayana. *J. Coord. Chem.*, **65**, 474 (2012).